NASA TECHNICAL NOTE

NASA TN D-4636

NASA TN D-4636

CORRELATION STUDY OF LUNAR RADII OBTAINED FROM PHOTOGRAPHIC AND LUNAR GRAVITATIONAL FIELD DATA

by James R. Williams and William R. Wells

Langley Research Center
Langley Station, Hampton, Va.

NATIONAL AERONAUTICS AND SPACE ADMINISTRATION • WASHINGTON, D. C. • JULY 1968

NASA TN D-4636

CORRELATION STUDY OF LUNAR RADII OBTAINED FROM PHOTOGRAPHIC AND LUNAR GRAVITATIONAL FIELD DATA

By James R. Williams and William R. Wells

Langley Research Center
Langley Station, Hampton, Va.

NATIONAL AERONAUTICS AND SPACE ADMINISTRATION

For sale by the Clearinghouse for Federal Scientific and Technical Information
Springfield, Virginia 22151 – CFSTI price $3.00

CORRELATION STUDY OF LUNAR RADII OBTAINED FROM PHOTOGRAPHIC AND LUNAR GRAVITATIONAL FIELD DATA

By James R. Williams and William R. Wells
Langley Research Center

SUMMARY

A study has been made to determine the correlation of local lunar radii as determined from recent earth-based photographic studies and from lunar gravitational field coefficients obtained from lunar satellite tracking data. The photographic study is a recent local radii determination performed by the Army Map Service at 734 points over the visible lunar surface. The lunar gravitational field coefficients used in the analysis are the most recent determinations from independent studies of tracking data from Lunar Orbiters I to IV and the Russian satellite LUNA-10.

The general result of the study is that all the currently determined gravity models are little correlated with the visible surface features of the moon except in a few isolated regions.

INTRODUCTION

Recently, new scientific data concerning the physical properties of the moon were obtained. The successful performance of the Lunar Orbiter series of spacecraft has made available preliminary estimates of the gravitational field of the moon (refs. 1 to 4 and unpublished data from the Langley Space Mechanics Division). At the same time, earth-based photographic studies of the figure of the moon have been made by the Army Map Service (ref. 5). It is possible to study the relation between these two independent data types (photographic and tracking data) by a comparison of lunar radii implied by the two methods. The comparison is made through a computation of the correlation coefficients of the two independently determined sets of lunar radii in various regions of the lunar surface. The values of the radii in each region as determined from either photographic measurements or a lunar gravitational model are considered to be random measurements of a representative radius for the region. The regions considered represent isolated maria regions and isolated mountainous regions as well as combinations of the two. In addition, the entire visible hemisphere is considered together with a region along the equator between $\pm 12^{\circ}$ latitude over which much of the data from the Lunar Orbiter satellites were obtained.

In order to calculate the lunar radii implied by the lunar gravitational field, it was necessary to convert the gravitational coefficients to equivalent surface coefficients as outlined in reference 6. This conversion requires an assumption on the internal density distribution of the moon. For the purposes of this analysis, the lunar density distribution is assumed to be uniform throughout.

In general, the correlation coefficient between two sets of random variables is a measure of the linear dependence of the random variables. For the problem treated in this paper, the random variables are the measured and computed radii at various points inside a particular region on the moon. With the assumption of a uniformly dense lunar interior, a high value of the correlation coefficient would indicate a definite relation of the surface features to the gravitational anomalies, whereas a low correlation would imply little dependence of these two quantities.

SYMBOLS

$C_{n,m}, S_{n,m}$ coefficients of lunar gravitational potential spherical harmonics (n is degree, m is order)

$E[X]$ expectation value of X

$F_{n,m}, H_{n,m}$ coefficients of lunar surface spherical harmonics (n is degree, m is order)

$h(\phi,\lambda)$ local deviation of surface shape from sphere

M mass of moon

N number of measurements

$P_{n,m}$ associated Legendre function (n is degree, m is order)

r distance from center of mass of moon to an external field point

R_o mean radius of moon

R_1 local radius of moon determined from earth-based photographic studies

R_2 local radius of moon determined from gravitational field

$R_{1,k}, R_{2,k}$ kth values of local lunar radii

r' distance from center of mass of moon to an interior point

U lunar gravitational potential function

X, Y random variables

α angle defined in sketch 1 in appendix

λ selenographic longitude of point on lunar surface

μ product of universal gravitational constant and mass of moon

$\mu_{XY}, \mu_{R_1R_2}$ covariances associated with X and Y and R_1 and R_2

$\rho_{XY}, \rho_{R_1R_2}$ correlation coefficients between X and Y and R_1 and R_2

$\sigma_X, \sigma_Y, \sigma_{R_1}, \sigma_{R_2}$ standard deviations of X and Y and R_1 and R_2

ϕ selenographic latitude of point on lunar surface

A bar over a quantity denotes the mean or expectation value of that quantity.

GENERAL CONSIDERATIONS

A study of the relation between two recently acquired independent data types concerning physical properties of the moon has been made. In the study it was convenient to relate the lunar gravitational field data type to equivalent lunar radii. This set of radii was then compared to the set of radii derived from earth-based photographic studies (ref. 5) by means of a correlation study.

Lunar Models

The preliminary estimates of the gravitational field considered consist primarily of the results of analyses of the tracking data from the Lunar Orbiter series of satellites (refs. 1 to 3 and unpublished data from the Langley Space Mechanics Division). The models in references 1 and 2 were obtained through a direct analysis of the tracking data from the satellites. The model in reference 2 is a refinement of the model in reference 1. The second of these models has additional tracking data which were obtained from a wide

variety of orbit configurations. The model in reference 3 and the one from the unpublished data are from independent studies which were obtained from long-period analyses of these tracking data. An additional model supplied by the Russian results from LUNA-10 as given in reference 4 is also considered.

The standard form of the lunar gravitational potential function as suggested by the International Astronomical Union (ref. 7) is

$$U(r,\phi,\lambda) = \frac{\mu}{r}\left[1 + \sum_{n=2}^{\infty}\sum_{m=0}^{n}\left(\frac{R_o}{r}\right)^n\left(C_{n,m}\cos m\lambda + S_{n,m}\sin m\lambda\right)P_{n,m}(\sin\phi)\right] \tag{1}$$

where r, ϕ, and λ are the spherical polar coordinates of the satellite relative to the center of mass of the moon, and $C_{n,m}$ and $S_{n,m}$ are the gravity coefficients. Numerical values for these coefficients, for the various models, are given in table I. Dashes in the table imply that a particular coefficient was not determined in the referenced work.

Lunar Radii

A local lunar radius can be calculated from gravity considerations provided the internal density distribution and the gravitational coefficients are known. At the present time, the exact degree of nonuniformity of the lunar density is not known but is expected to be small. For this reason, the assumption of constant density was made in this analysis. With this assumption the value for the local lunar radii is obtained from the following equation as given in reference 6:

$$R_2(\phi,\lambda) = R_o\left[1 + \sum_{n=2}^{\infty}\sum_{m=0}^{n}\left(\frac{2n+1}{3}\right)\left(C_{n,m}\cos m\lambda + S_{n,m}\sin m\lambda\right)P_{n,m}(\sin\phi)\right] \tag{2}$$

where ϕ and λ are the selenographic latitude and longitude of a local point on the lunar surface, and $C_{n,m}$ and $S_{n,m}$ are the gravity coefficients discussed previously. A brief derivation of this result is given in the appendix.

Correlation Coefficient

The correlation coefficient is a measure of the interdependence of two random variables X and Y. A value of ± 1 implies that the two variables are related to each other linearly, whereas a value of zero generally implies that no linear relationship exists between the variables. The usual definition of the correlation coefficient between X and Y is

$$\rho_{XY} = \frac{\mu_{XY}}{\sigma_X\sigma_Y} \tag{3}$$

where

$$\left.\begin{aligned} \mu_{XY} &= E\left[(X - \bar{X})(Y - \bar{Y})\right] \\ \sigma_X^2 &= E\left[(X - \bar{X})^2\right] \\ \sigma_Y^2 &= E\left[(Y - \bar{Y})^2\right] \end{aligned}\right\} \tag{4}$$

and

$$\left.\begin{aligned} \bar{X} &= E[X] \\ \bar{Y} &= E[Y] \end{aligned}\right\} \tag{5}$$

A more complete discussion of the correlation coefficient and variances and covariances of X and Y can be found in reference 8.

Correlation Coefficient for the Lunar Radii

In this analysis, the local lunar radii R_1 and R_2 as determined from photographic and gravitational data are treated as random variables. If R_1 and R_2 are used in place of X and Y in the equations of the previous section, the values of $\mu_{R_1R_2}$, σ_{R_1}, and σ_{R_2} are

$$\left.\begin{aligned} \mu_{R_1R_2} &= \sum_{k=1}^{N} \frac{(R_{1,k} - \bar{R}_1)(R_{2,k} - \bar{R}_2)}{N - 1} \\ \sigma_{R_1}^2 &= \sum_{k=1}^{N} \frac{(R_{1,k} - \bar{R}_1)^2}{N - 1} \\ \sigma_{R_2}^2 &= \sum_{k=1}^{N} \frac{(R_{2,k} - \bar{R}_2)^2}{N - 1} \end{aligned}\right\} \tag{6}$$

and

$$\left.\begin{aligned} \bar{R}_1 &= \sum_{k=1}^{N} \frac{R_{1,k}}{N} \\ \bar{R}_2 &= \sum_{k=1}^{N} \frac{R_{2,k}}{N} \end{aligned}\right\} \tag{7}$$

where N is the number of measured values of the radius in any particular region on the moon, and $R_{1,k}$ and $R_{2,k}$ are the kth values of a measurement of R_1 and R_2, respectively. Substituting equations (6) and (7) into equation (3) gives the following expression for the correlation coefficient between the two radii determinations (replacing X and Y by R_1 and R_2):

$$\rho_{R_1R_2} = \frac{\sum_{k=1}^{N} \left(R_{1,k} - \bar{R}_1\right)\left(R_{2,k} - \bar{R}_2\right)}{\left[\sum_{k=1}^{N} \left(R_{1,k} - \bar{R}_1\right)^2\right]^{1/2} \left[\sum_{k=1}^{N} \left(R_{2,k} - \bar{R}_2\right)^2\right]^{1/2}} \tag{8}$$

Values of the correlation coefficient as given by equation (8) were computed for the radii determined from the five lunar gravitational models designated models L-1 to L-5 in table I, and the 734 lunar radii determined by the Army Map Service in reference 5.

ANALYSIS AND RESULTS

For the purposes of this analysis the visible lunar surface was divided into various regions which represent both maria and mountainous terrain. In addition, a region between $\pm 12^{\circ}$ latitude and extending across the visible side is considered as well as the entire visible hemisphere. For each of the regions, the correlation between the lunar radii implied by earth-based photographic studies and that implied by the lunar gravitational coefficients was computed. In this analysis, surface features are considered highly correlated with the local gravitational field in any region for which the magnitude of the correlation coefficient is greater than 0.50. The results of the calculation for each of the gravity models L-1 to L-5 are given in table II for each region on the lunar surface. These regions, together with their corresponding correlations, are shown on the lunar maps in figures 1 to 5.

The numbers in the first row of table II give an indication of the general correlation between the radii from the two data types. These numbers represent the overall correlation coefficient for each gravity model. The highest overall correlation of 0.36, based on the entire 734 measurements, is obtained from model L-3 which was determined from Lunar Orbiter I data. The next highest overall value of 0.32 is obtained from model L-2 which was determined from a study utilizing a large amount of tracking data and a wide variety of orbit configurations. However, for the region between $\pm 12^{\circ}$ latitude and across the visible hemisphere (row two in table II), model L-2 has a correlation of 0.40 while model L-3 has a correlation of 0.22.

Regions 1 to 10 are located primarily in the various maria on the visible hemisphere. Taken together, these regions represent 164 individual photographic measurements of the lunar radius with some regions having as few as five and some having as many as 39 measurements. In regions 2 and 3, where more than half the maria region measurements are made, the gravity models are poorly correlated with the surface features.

Regions 11 to 14 are located primarily in various mountainous ranges on the visible hemisphere. These regions represent a total of 183 measurements. Of the five models considered, model L-3 has the most consistent correlation in all four of these mountainous regions. The correlation coefficient for model L-3 varies from a low of 0.25 in region 14 to a high of 0.50 in region 13. Regions 11 and 12 represent more radius measurements than do regions 13 and 14 and, consequently, serve as the better indication of the degree of correlation in these regions.

CONCLUDING REMARKS

A study has been conducted to determine the correlation between the lunar radii as determined from earth-based photographic studies and from the lunar gravity field determined from lunar satellite tracking data. With the exception of a few isolated regions on the moon, the gravity models were poorly correlated (a correlation coefficient less than 0.50) with the surface features represented by photographic data. Of the five gravity models considered, the model designated L-3 has the largest correlation (0.36) for the entire visible hemisphere. This low value indicates, on the average, a poor correlation between the visible surface features and the gravitational field. The correlation coefficients varied considerably with the gravity model in the designated maria and mountainous regions. However, for all models, the correlation was generally low in each type of terrain with the exception of a few isolated values.

At the present time, it appears likely that neither of the five preliminary gravity models L-1 to L-5 represents exactly the true lunar gravitational field. For this reason, it cannot be said definitely whether the correlation coefficients obtained in this analysis are physically meaningful. It is interesting to note, however, that the analysis on each model implies little correlation of the lunar surface features (lunar radii) with the lunar gravity field.

Langley Research Center,
National Aeronautics and Space Administration,
Langley Station, Hampton, Va., March 21, 1968,
129-04-01-01-23.

APPENDIX

CALCULATION OF THE LUNAR RADIUS

The surface equation for a body of uniform density can be obtained from its gravitational potential function expressed in the form

$$U(r,\phi,\lambda) = \frac{\mu}{M}\int_M \frac{dM}{\left(r'^2 + r^2 - 2r'r\cos\alpha\right)^{1/2}} \tag{A1}$$

where the quantities r', r, and α are illustrated in the following sketch:

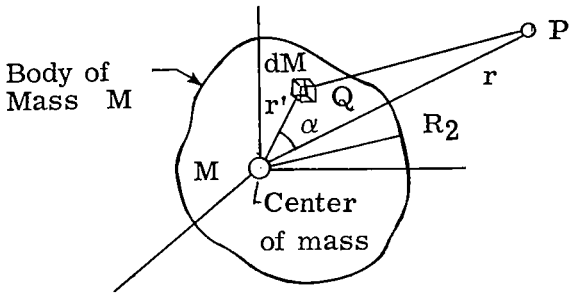

Sketch 1

The denominator of the integrand in equation (A1) can be expressed in terms of Legendre polynomials resulting in

$$U(r,\phi,\lambda) = \frac{\mu}{r}\left[1 + \frac{1}{M}\sum_{n=2}^{\infty}\frac{1}{r^n}\int_M r'^n P_n(\cos\alpha)\,dM\right] \tag{A2}$$

The Legendre polynomial $P_n(\cos\alpha)$ can be further expanded in terms of spherical harmonics as

$$P_n(\cos\alpha) = P_n(\sin\phi)P_n(\sin\phi') + 2\sum_{m=1}^{n}\left[\frac{(n-m)!}{(n+m)!}P_{n,m}(\sin\phi)P_{n,m}(\sin\phi')\cos m(\lambda - \lambda')\right] \tag{A3}$$

where ϕ and λ are the latitude and longitude, respectively, of the external point P in sketch 1 and ϕ' and λ' are the latitude and longitude of the interior point Q. The element of mass dM can be expressed in terms of a mean density σ and the latitude and longitude of point Q as

$$dM = \sigma r'^2\cos\phi'\,dr'\,d\phi'\,d\lambda' \tag{A4}$$

Substitution of equation (A4) into equation (A2) results in

APPENDIX

$$U(r,\phi,\lambda) = \frac{\mu}{r}\left[1 + \frac{\sigma}{M}\sum_{n=2}^{\infty}\frac{1}{r^n}\int_{-\pi/2}^{\pi/2}\int_{0}^{2\pi}\int_{0}^{R_2(\phi',\lambda')} r'^{\,n+2}\cos\phi' P_n(\cos\alpha)\,dr'\,d\lambda'\,d\phi'\right] \tag{A5}$$

Equation (A5) can be integrated with respect to the variable r' to obtain

$$U(r,\phi,\lambda) = \mu\left[1 + \frac{\sigma}{M}\sum_{n=2}^{\infty}\frac{1}{(n+3)r^n}\int_{-\pi/2}^{\pi/2}\int_{0}^{2\pi}\left[R_2(\phi',\lambda')\right]^{n+3}\cos\phi' P_n(\cos\alpha)\,d\lambda'\,d\phi'\right] \tag{A6}$$

The equation of the surface $R_2(\phi,\lambda)$ can be written in terms of a mean value R_o plus some small perturbation about this value as follows:

$$R_2(\phi,\lambda) = R_o\left[1 + h(\phi,\lambda)\right] \tag{A7}$$

where $|h| \ll 1$. To a first approximation

$$\left[R_2(\phi,\lambda)\right]^{n+3} = R_o^{\,n+3}\left[1 + (n+3)h(\phi,\lambda)\right] \tag{A8}$$

Substitution of the value given by equation (A8) for R_2^{n+3} into U in equation (A6) results in

$$U(r,\phi,\lambda) = \frac{\mu}{r}\left[1 + \frac{\sigma R_o^{\,3}}{M}\sum_{n=2}^{\infty}\frac{1}{n+3}\left(\frac{R_o}{r}\right)^n\int_{-\pi/2}^{\pi/2}\int_{0}^{2\pi}\cos\phi' P_n(\cos\alpha)\,d\lambda'\,d\phi'\right.$$

$$\left. + \frac{\sigma R_o^{\,3}}{M}\sum_{n=2}^{\infty}\left(\frac{R_o}{r}\right)^n\int_{-\pi/2}^{\pi/2}\int_{0}^{2\pi} h(\phi',\lambda')\cos\phi' P_n(\cos\alpha)\,d\lambda'\,d\phi'\right] \tag{A9}$$

It can be shown from the orthogonal properties of Legendre polynomials that the first infinite series in equation (A9) vanishes. This gives

$$U(r,\phi,\lambda) = \frac{\mu}{r}\left[1 + \frac{\sigma R_o^{\,3}}{M}\sum_{n=2}^{\infty}\left(\frac{R_o}{r}\right)^n\int_{-\pi/2}^{\pi/2}\int_{0}^{2\pi} h(\phi',\lambda')\cos\phi' P_n(\cos\alpha)\,d\lambda'\,d\phi'\right] \tag{A10}$$

At this point it is convenient to expand $h(\phi,\lambda)$ in terms of spherical harmonics as follows:

$$h(\phi,\lambda) = \sum_{k=2}^{\infty}\sum_{p=0}^{k}\left(F_{k,p}\cos p\lambda + H_{k,p}\sin p\lambda\right)P_{k,p}(\sin\phi) \tag{A11}$$

where the surface coefficients $F_{k,p}$ and $H_{k,p}$ depend on the function of h. Substitution of this result into equation (A10) together with the value for $P_n(\cos \alpha)$ as given by equation (A3) and integrating with respect to ϕ' and λ' gives

$$U(r,\phi,\lambda) = \frac{\mu}{r}\left[1 + \frac{4\pi R_o{}^3\sigma}{M}\sum_{n=2}^{\infty}\sum_{m=0}^{n}\left(\frac{R_o}{r}\right)^n\left(\frac{1}{2n+1}\right)\left(F_{n,m}\cos m\lambda + H_{n,m}\sin m\lambda\right)P_{n,m}(\sin\phi)\right] \tag{A12}$$

If R_o is determined from the condition that

$$\frac{4\pi R_o{}^3\sigma}{3} = M \tag{A13}$$

then,

$$U(r,\phi,\lambda) = \frac{\mu}{r}\left[1 + \sum_{n=2}^{\infty}\sum_{m=0}^{n}\left(\frac{R_o}{r}\right)^n\left(\frac{3}{2n+1}\right)\left(F_{n,m}\cos m\lambda + H_{n,m}\sin m\lambda\right)P_{n,m}(\sin\phi)\right] \tag{A14}$$

A direct comparison with the form of the potential function as given by equation (A14) with that given in the standard form in terms of gravity coefficients, that is

$$U(r,\phi,\lambda) = \frac{\mu}{r}\left[1 + \sum_{n=2}^{\infty}\sum_{m=0}^{n}\left(\frac{R_o}{r}\right)^n\left(C_{n,m}\cos m\lambda + S_{n,m}\sin m\lambda\right)P_{n,m}(\sin\phi)\right] \tag{A15}$$

indicates that the surface coefficients are related to the gravity coefficients as

$$\left.\begin{aligned} F_{n,m} &= \frac{2n+1}{3}C_{n,m} \\ H_{n,m} &= \frac{2n+1}{3}S_{n,m} \end{aligned}\right\} \tag{A16}$$

This means that in the case of a constant density assumption the shape of the surface can be related to the gravitational field in the following manner:

$$R_2(\phi,\lambda) = R_o\left[1 + h(\phi,\lambda)\right] = R_o\left[1 + \sum_{n=2}^{\infty}\sum_{m=0}^{n}\left(F_{n,m}\cos m\lambda + H_{n,m}\sin m\lambda\right)P_{n,m}(\sin\phi)\right]$$

$$= R_o\left[1 + \sum_{n=2}^{\infty}\sum_{m=0}^{n}\left(\frac{2n+1}{3}\right)\left(C_{n,m}\cos m\lambda + S_{n,m}\sin m\lambda\right)P_{n,m}(\sin\phi)\right] \tag{A17}$$

This result agrees with that given in reference 9 in which this expression is stated but not derived.

REFERENCES

1. Michael, William H., Jr.; Tolson, Robert H.; and Gapcynski, John P.: Preliminary Results on the Gravitational Field of the Moon From Analysis of Lunar Orbiter Tracking Data. Paper presented at the American Geophysical Union Annual Meeting (Washington, D. C.), Apr. 17-20, 1967.

2. Tolson, Robert H.; and Gapcynski, John P.: An Analysis of the Lunar Gravitational Field as Obtained From Lunar Orbiter Tracking Data. Paper presented at the IQSY/COSPAR Assemblies (London, England), July 17-28, 1967.

3. Lorell, J.; and Sjogren, W. L.: Preliminary Lunar Gravity Estimates From Lunar Orbiter. Supporting Research and Advanced Development, Space Programs Summary 37-46, Vol. IV (Contract No. NAS7-100), Jet Propulsion Lab., California Inst. Technol., Aug. 31, 1967, pp. 1-5.

4. Akim, E. L.: Determination of the Gravitational Field of the Moon by Motion of AMS LUNAR-10. ST-CM-LPS-10532 (Contract NAS5-12487), Volt Tech. Corp., Nov. 2, 1966. (Transl. from Dokl. Akad. Wauk SSSR, vol. 170, no. 4, 1966, pp. 799-802.)

5. Army Map Serv.; and Aeronaut. Chart Inform. Center: Department of Defense Selenodetic Control System 1966. Tech. Rep. No. 1, Def. Intel. Agency, Jan. 1967. (Available from DDC as AD 648067.)

6. Wells, William R.: Notes on Gravitational Potential Theory. Eng. Ext. Ser. Circ. No. 6, Virginia Polytech. Inst., [1966].

7. Anon: Commission de la mecanique celeste. Transactions of the International Astronomical Union. Vol. XI B – Proceedings of the Eleventh General Assembly, D. H. Sadler, ed., Academic Press, 1962, pp. 171-174.

8. Laning,J. Halcombe, Jr.; and Battin, Richard H.: Random Processes in Automatic Control. McGraw-Hill Book Co., Inc., 1956.

9. Jeffreys, Harold. The Earth. Fourth ed., Cambridge Univ. Press, 1959, pp. 145-146.

TABLE I.- COEFFICIENTS OF PRELIMINARY ESTIMATES OF LUNAR GRAVITATIONAL FIELD

n,m	Model L-1 (ref. 1)		Model L-2 (ref. 2)		Model L-3 (Unpublished data from Langley Space Mechanics Division)		Model L-4 (ref. 3)		Model L-5 (ref. 4)	
	$C_{n,m}$	$S_{n,m}$	$C_{n,m}$	$S_{n,m}$	$C_{n,m}$	$S_{n,m}$	$C_{n,m}$	$S_{n,m}$	$C_{n,m}$	$S_{n,m}$
2,0	-2.2187×10^{-4}	----------	-2.0596×10^{-4}	----------	-2.3691×10^{-4}	----------	-1.9244×10^{-4}	----------	-2.06×10^{-4}	----------
2,1	.1250	0.2145×10^{-4}	-.1661	0.0080×10^{-4}	.0445	-0.0363×10^{-4}	-.0897	0.0363×10^{-4}	.157	0.036×10^{-4}
2,2	.3204	-.3052	.2042	-.0342	.2852	.1027	.2241	.1527	.140	-.014
3,0	.2943	----------	-.3773	----------	.3366	----------	-.5911	----------	-.363	----------
3,1	.2350	.3934	.3012	.1762	.3809	.1115	.3585	.0991	-.568	-.178
3,2	.1933	.1440	.1294	-.0147	.0285	.0064	-.0421	-.0071	.118	-.007
3,3	-.0317	.0831	.0317	-.0043	.1532	.0537	-.0217	-.0713	----------	----------
4,0	-.0418	----------	.0798	----------	-.1368	----------	.1843	----------	.333	----------
4,1	.0163	.1908	-.1560	.0391	----------	----------	-.1391	.0764	----------	----------
4,2	-.0276	-.1035	.0011	.0072	----------	----------	.0259	-.0107	----------	----------
4,3	.0179	.0076	-.0082	-.0001	----------	----------	.0154	-.0260	----------	----------
4,4	-.0014	-.0147	-.0007	.0011	----------	----------	.0084	.0089	----------	----------
5,0	----------	----------	-.5505	----------	----------	----------	-.5751	----------	----------	----------
5,1	-.1274	.1951	-.0385	.0829	----------	----------	----------	----------	----------	----------
5,2	.0809	-.0015	.0342	-.0203	----------	----------	----------	----------	----------	----------
5,3	-.0102	.0058	-.0071	-.0078	----------	----------	----------	----------	----------	----------
5,4	.0030	-.0044	-.0008	-.0013	----------	----------	----------	----------	----------	----------
5,5	-.0009	.0017	-.0003	.0003	----------	----------	----------	----------	----------	----------
6,0	----------	----------	----------	----------	----------	----------	.0479	----------	----------	----------
7,0	----------	----------	----------	----------	----------	----------	.0905	----------	----------	----------

TABLE II.- CORRELATION COEFFICIENTS FOR PRELIMINARY GRAVITATIONAL MODELS

Region	$\rho_{R_1R_2}$ for model –					N
	L-1	L-2	L-3	L-4	L-5	
Visible hemisphere	0.23	0.32	0.36	0.23	0.14	734
Equatorial region	.35	.40	.22	.06	-.17	22
1	.53	-.22	-.35	-.07	.52	14
2	.16	.33	.31	-.12	.43	39
3	-.15	.18	-.10	.22	.29	29
4	-.08	-.05	.04	.10	-.10	6
5	.13	-.30	.25	.60	-.52	19
6	-.39	-.38	-.20	-.24	-.18	22
7	-.57	.52	.62	-.68	.07	5
8	.07	-.47	.16	.25	-.16	15
9	.07	.22	-.10	.05	-.02	10
10	-.12	-.25	.27	-.39	-.51	5
11	.20	.30	.44	.27	.27	67
12	.24	.42	.41	-.10	.54	84
13	.05	-.01	.50	.16	.07	12
14	-.04	-.12	.25	.12	.25	20

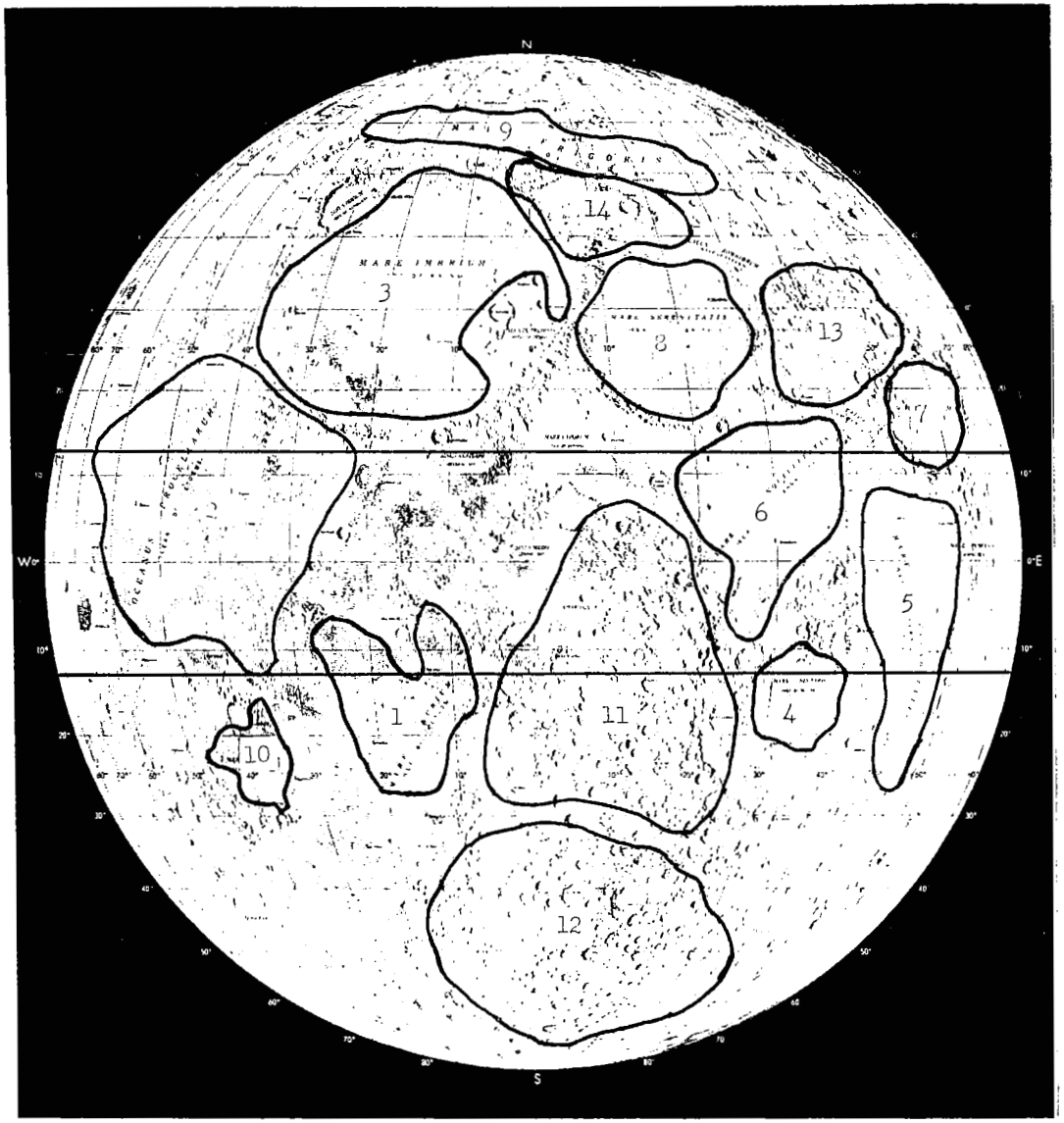

Region	$\rho_{R_1R_2}$	N
Visible Hemisphere	0.23	734
Equatorial Region	0.35	22
1	0.53	14
2	0.16	39
3	-0.15	29
4	-0.08	6
5	0.13	19
6	-0.39	22
7	-0.57	5
8	0.07	15
9	0.07	10
10	-0.12	5
11	0.20	67
12	0.24	84
13	0.05	12
14	-0.04	20

Figure 1.- Correlations for model L-1.

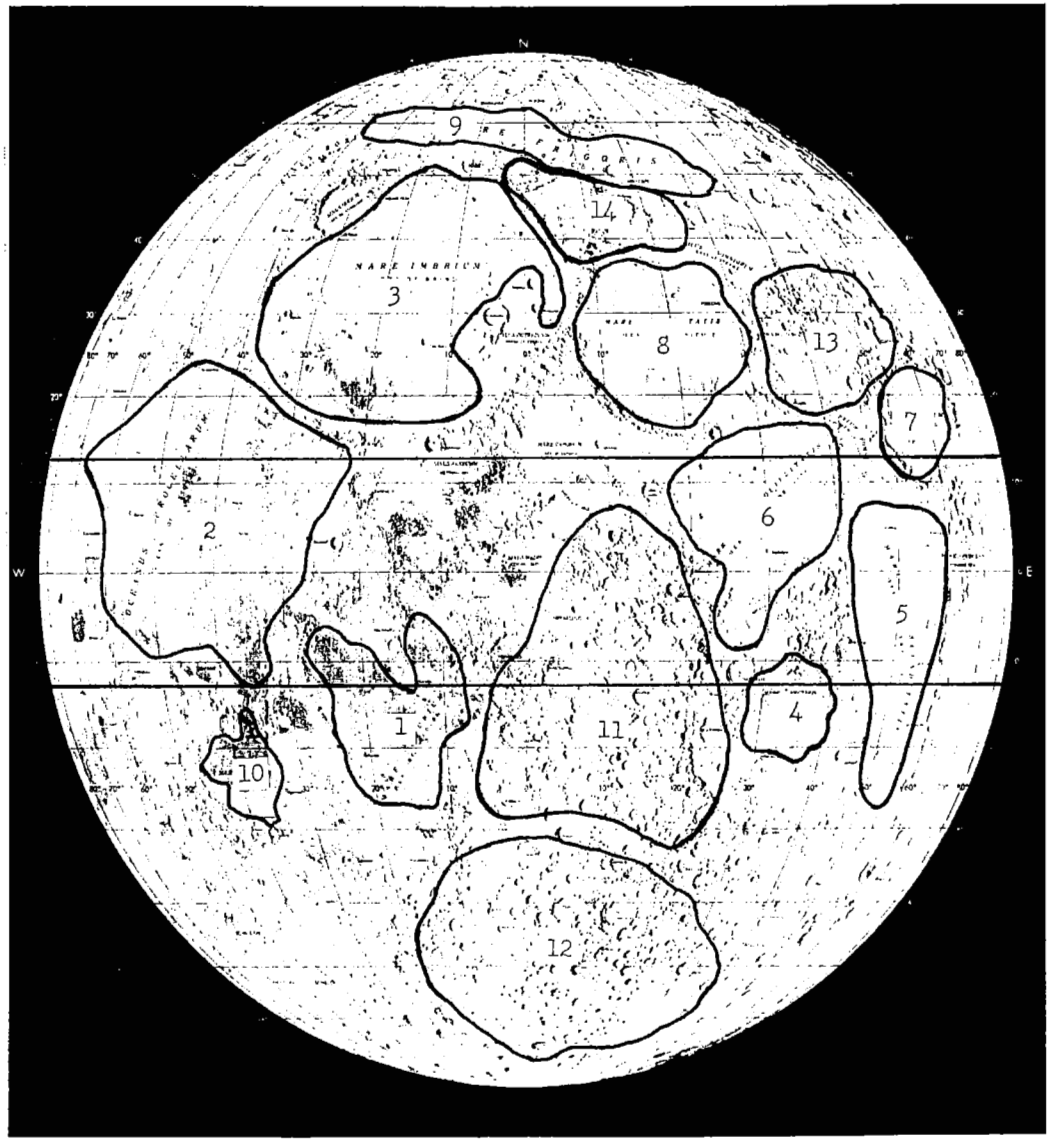

Region	$\rho_{R_1R_2}$	N
Visible Hemisphere	0.32	734
Equatorial Region	0.40	22
1	-0.22	14
2	0.33	39
3	0.18	29
4	-0.05	6
5	-0.30	19
6	-0.38	22
7	0.52	5
8	-0.47	15
9	0.22	10
10	-0.25	5
11	0.30	67
12	0.42	84
13	-0.01	12
14	-0.12	20

Figure 2.- Correlations for model L-2.

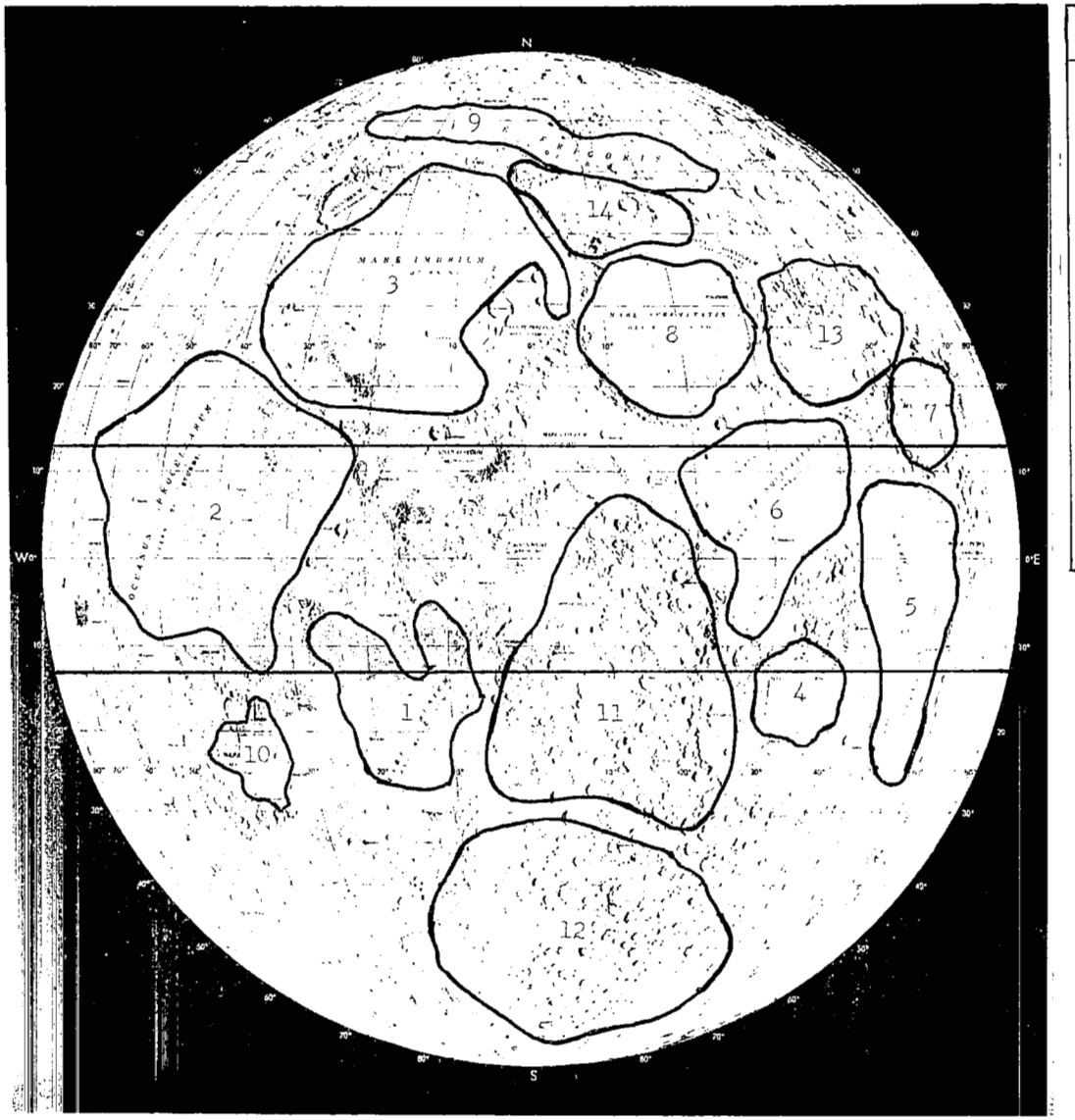

Region	$\rho_{R_1R_2}$	N
Visible Hemisphere	0.36	734
Equatorial Region	0.22	22
1	-0.35	14
2	0.31	39
3	-0.10	29
4	0.04	6
5	0.25	19
6	-0.20	22
7	0.62	5
8	0.16	15
9	-0.10	10
10	0.27	5
11	0.44	67
12	0.41	84
13	0.50	12
14	0.25	20

Figure 3.- Correlations for model L-3.

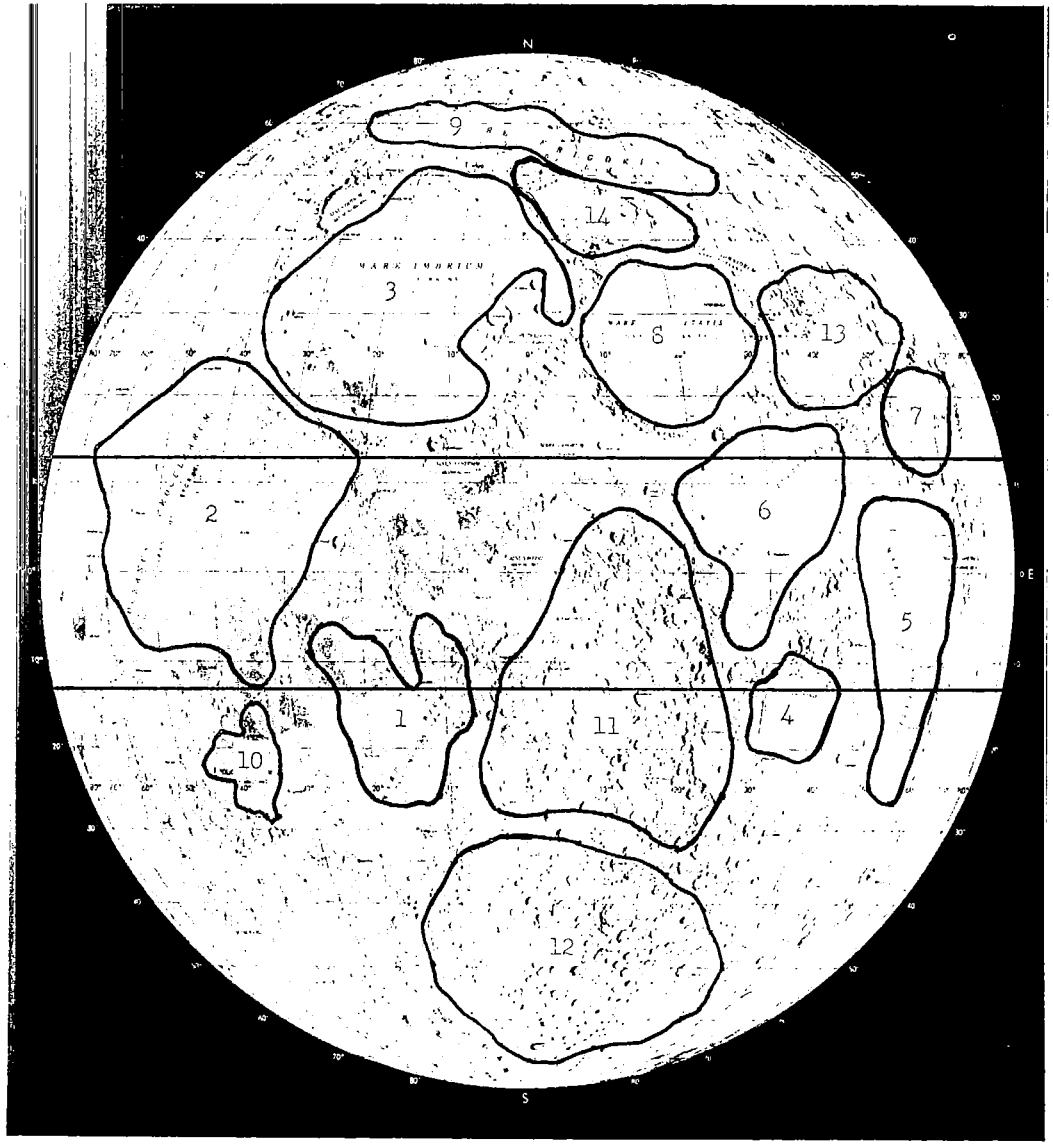

Region	$\rho_{R_1 R_2}$	N
Visible Hemisphere	0.23	734
Equatorial Region	0.06	22
1	-0.07	14
2	-0.12	39
3	0.22	29
4	0.10	6
5	0.60	19
6	-0.24	22
7	-0.68	5
8	0.25	15
9	0.05	10
10	-0.39	5
11	0.27	67
12	-0.10	84
13	0.16	12
14	0.12	20

Figure 4.- Correlations for model L-4.

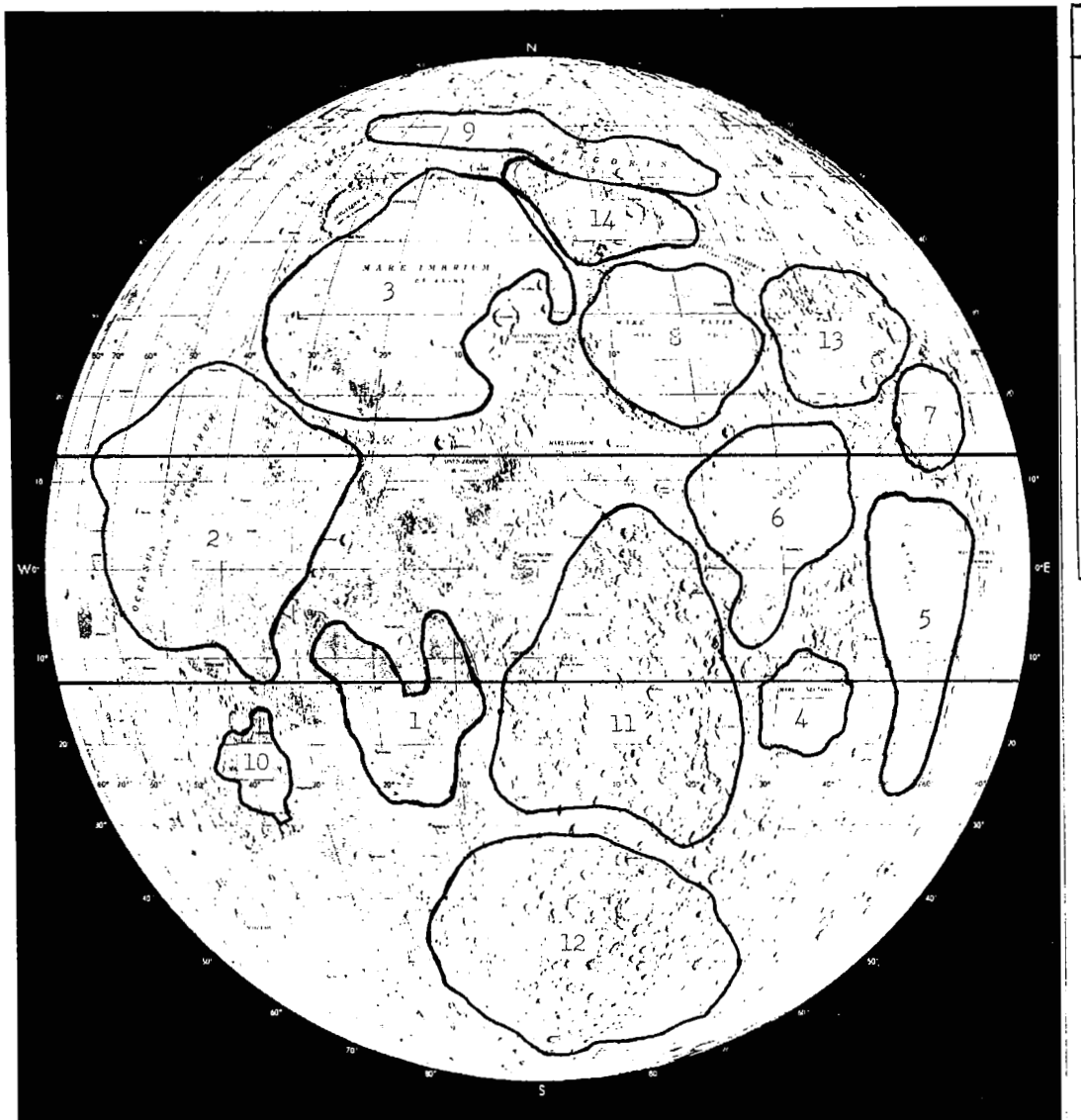

Region	$\rho_{R_1R_2}$	N
Visible Hemisphere	0.14	734
Equatorial Region	-0.17	22
1	0.52	14
2	0.43	39
3	0.29	29
4	-0.10	6
5	-0.52	19
6	-0.18	22
7	0.07	5
8	-0.16	15
9	-0.02	10
10	-0.51	5
11	0.27	67
12	0.54	84
13	0.07	12
14	0.25	20

Figure 5.- Correlations for model L-5.